

Calorimetry-Application

COMPUTER SIMULATION OF THERMAL ANALYSIS IN HEAT-FLUX DSC APPLIED TO METAL SOLIDIFICATION

R. Ciach, W. Kapturkiewicz**, W. Wolczyński* and A. M. Zahra****

*INSTITUTE FOR METAL RESEARCH, POLISH ACADEMY OF SCIENCES, 30 059
KRAKÓW, REYMONTA 25, POLAND

**FACULTY OF FOUNDRY, ACADEMY OF MINING AND METALLURGY, 30 059
KRAKÓW, REYMONTA 23, POLAND

***CENTRE DE THERMODYNAMIQUE ET DE MICROCALORIMÉTRIE, CENTRE
NATIONAL DE LA RECHERCHE SCIENTIFIQUE, 13 003 MARSEILLE, 26, RUE DU 141e
R.I. A., FRANCE

A general mathematical treatment for heat-flux differential scanning calorimetry is given. It combines equations derived for heat transfer in the calorimeter cell with an approach to the solidification of metal or alloy carried out in this type of instrument. The differences are discussed between temperature evolution, kinetics of latent heat and undercooling evolution within the sample, and temperature evolution, recorded signal and measured undercooling at the monitoring station.

Keywords: alloys, heat-flux differential scanning calorimetry, kinetics, metals

Introduction

Differential scanning calorimetry allows the study of thermal effects which accompany the solidification of a metal or alloy. The overall thermal effect is equivalent to the enthalpy of the process being studied. Owing to the sample temperature lag, however, the curve does not correctly represent the considered kinetics.

The proposed use of a mathematical model for heat transfer in the DSC cell, combined with an approach to nucleation and crystal growth, is one of the possible ways to

John Wiley & Sons, Limited, Chichester
Akadémiai Kiadó, Budapest

reproduce the real kinetics of solidification. The analysis of heat transfer seems to be more realistic than that of the idealized Mraw model [1].

A solution to the derived set of equations is developed, analogously as done by Saito *et al.* [2] for Mraw's approach [1], in which only two separate resistances are considered.

The present outline of heat transfer corresponds to the construction principle applied in du Pont instruments, known as heat-flux differential scanning calorimetry.

The appropriate equations governing the analysed technique, shown schematically as a system of thermal resistances and capacities, are developed. The temperature within a sample at each instant of the process being studied is the parameter via which the above equations are coupled with another set of equations governing the non-stationary solidification of the metal or alloy.

This permits calculation of this temperature and also the temperature at the monitoring station. Moreover, both the kinetics of the thermal effect in the sample and the signal from the monitoring station can be simulated.

The current analysis considers the temperature evolution in the heater as the boundary conditions. Thus, the calculations do not require a knowledge of the recorded signal. The signal can be obtained by means of theoretical calculations, and then compared with the measured one.

A temperature gradient in the sample is neglected in the present analysis.

The purpose of the proposed work is to prove the difference between the kinetics of the thermal effect within the sample and the signal monitored during DSC measurements.

General considerations

The proposed analysis considers solidification in the heat-flux differential scanning calorimeter and Fig. 1 outlines the Du Pont instrument which employs this principle of measurement. The respective calculations have been developed on the basis of the outline.

Modelling of non-stationary capacity-resistance system for heat-flux DSC

The DSC cell shown schematically in Fig. 1 was used in the investigations carried out by Pulluard [3].

The scheme of heat transfer in the DSC cell is shown in Fig. 2a, and the system of heat resistances and capacities in Fig. 2b.

The following symbols are used in the sketch:

T_i = temperature points, ($i = 1, \dots, 7$),

C_i = heat capacities, J/K, ($i = 2, \dots, 6$); $C_i = c_i \cdot \rho_i \cdot V_i$,

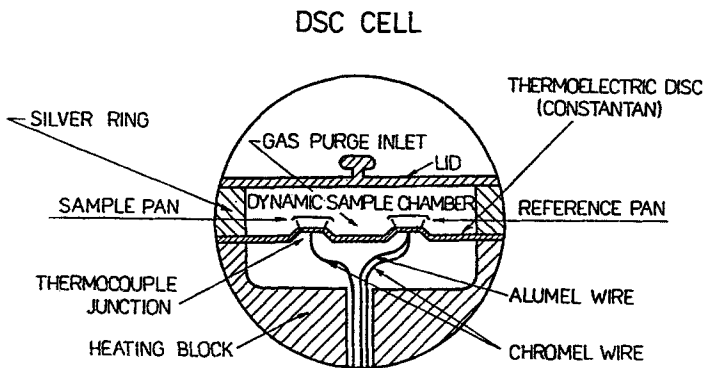


Fig. 1 Measurement principle of the Du Pont instrument

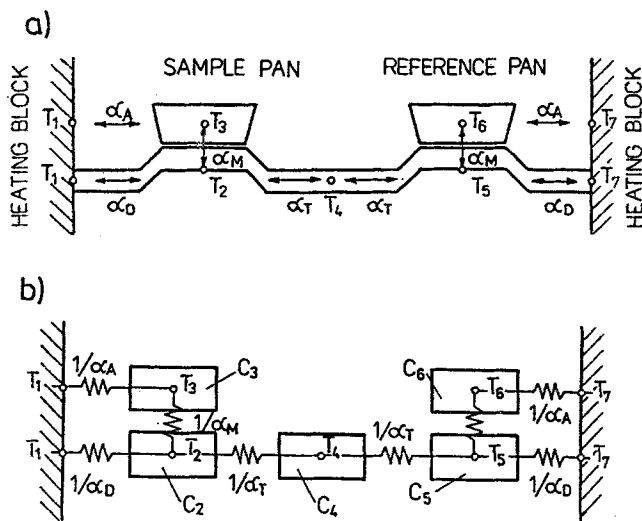


Fig. 2 Sketch of calorimeter cell: a) heat transfer in the DSC cell, b) system of heat capacities and resistances.

Arrows denote directions of heat fluxes for cooling or heating

c_i, ρ_i, V_i = specific heat, $J/(g \cdot K)$, density, g/cm^3 , and volume of system element, cm^3 , respectively,

α_J = effective coefficient of heat transfer, W/K , ($J = A, D, M, T$),

$1/\alpha_A$ = heat resistance between heater and samples (through atmosphere of cell),

- $1/\alpha_D$ = heat resistance of part of disc between heater and measurement points T_2 and T_5 ,
 $1/\alpha_M$ = heat resistance between samples and measurement points T_2 and T_5 ,
 $1/\alpha_T$ = heat resistance of part of disc between measurement points T_2 and T_5 , and temperature point T_4 .

Elementary thermal balance for calorimeter cell

According to the system of resistances and capacities shown in Fig. 2b, the following set of equations may be written:

$$(T_1 - T_2) * \alpha_D * \Delta t + (T_3 - T_2) * \alpha_M * \Delta t + (T_4 - T_2) * \alpha_T * \Delta t = C_2 * (T_2^i - T_2) \quad (1a)$$

$$(T_1 - T_3) * \alpha_A * \Delta t + (T_2 - T_3) * \alpha_M * \Delta t = C_3 * (T_3^i - T_3) \quad (1b)$$

$$(T_2 - T_4) * \alpha_T * \Delta t + (T_5 - T_4) * \alpha_T * \Delta t = C_4 * (T_4^i - T_4) \quad (1c)$$

$$(T_4 - T_5) * \alpha_T * \Delta t + (T_6 - T_5) * \alpha_M * \Delta t + (T_7 - T_5) * \alpha_D * \Delta t = C_5 * (T_5^i - T_5) \quad (1d)$$

$$(T_5 - T_6) * \alpha_M * \Delta t + (T_7 - T_6) * \alpha_A * \Delta t = C_6 * (T_6^i - T_6) \quad (1e)$$

where Δt = time step, s,

T_i^i = temperature in current time step, °C, ($i = 1, \dots, 7$),

T_i = temperature in previous time step, °C, ($i = 1, \dots, 7$)

Rearrangement of Eqs (1) yields

$$T_2^i = T_2 * (1 - A_2 - B_2 - E_2) + A_2 * T_1 + B_2 * T_3 + E_2 * T_4 \quad (2a)$$

$$T_3^i = T_3 * (1 - A_3 - B_3) + A_3 * T_1 + B_3 * T_2 \quad (2b)$$

$$T_4^i = T_4 * (1 - A_4 - B_4) + A_4 * T_2 + B_4 * T_5 \quad (2c)$$

$$T_5^i = T_5 * (1 - A_5 - B_5 - E_5) + A_5 * T_4 + B_5 * T_6 + E_5 * T_7 \quad (2d)$$

$$T_6^i = T_6 * (1 - A_6 - B_6) + A_6 * T_5 + B_6 * T_7 \quad (2e)$$

where

$$A_2 = \alpha_D * \Delta t / C_2 \quad (3a)$$

$$A_3 = \alpha_M * \Delta t / C_3 \quad (3b)$$

$$A_4 = \alpha_T * \Delta t / C_4 \quad (3c)$$

$$A_5 = \alpha_T * \Delta t / C_5 \quad (3d)$$

$$A_6 = \alpha_M * \Delta t / C_6 \quad (3e)$$

$$B_2 = \alpha_M * \Delta t / C_2 \tag{3f}$$

$$B_3 = \alpha_A * \Delta t / C_3 \tag{3g}$$

$$B_4 = \alpha_T * \Delta t / C_4 \tag{3h}$$

$$B_5 = \alpha_M * \Delta t / C_5 \tag{3i}$$

$$B_6 = \alpha_A * \Delta t / C_6 \tag{3j}$$

$$E_2 = \alpha_T * \Delta t / C_2 \tag{3k}$$

$$E_5 = \alpha_D * \Delta t / C_5 \tag{3l}$$

and

$$T_1 = T_7 = T_0 + u_0 * \Delta t \tag{4}$$

T_0 = initial temperature of heater, °C,

u_0 = rate of change of heater temperature, deg/s.

The stability of the solution requires that

$$1 - A_i - B_i - E_i \geq 0 \tag{5}$$

where $i = 2, \dots, 6$ according to Eqs (3)

and for $i = 3, 4, 6, E_i = 0$

Mathematical treatment for solidification

A mathematical treatment for the solidification of a metal or alloy shown below relates the heat-flux DSC technique to the nucleation and crystal growth approach [4]. The sample is considered as one element with no temperature gradient inside, the product of solidification is one phase only, and certain parameters of nucleation and growth are constant:

$$c_s * \rho_s * V_s * dT_s/dt = \sum \alpha_i * F_i * (T_3 - T_i^e) + q * V_s \tag{6}$$

where

c_s, ρ_s = specific heat, J/(g K), and density, g/cm³, of sample, respectively,

T_i^e = environment temperature, °C, in i -direction of heat transfer,

α_i = heat transfer coefficient, W/(cm²K),

F_i = surface in i -direction of heat transfer, cm²,

V_s = volume of sample, cm³,

t = time, s ,

q = rate of latent heat evolution, W/cm^3 .

The following definition may be inserted into Eq. (6):

$$q = L * dV/dt \quad (7)$$

where V may be defined as predicted previously [5–7]:

$$V = 1 - \exp(-\Omega) \quad (8)$$

where

L = latent heat, J/cm^3 ,

V = volume fraction of solidified metal (undimensional),

and

$$\Omega = 4/3 * \Pi * N * \left(\int_0^t u * dt \right)^3 \quad (9)$$

where

N = number of grains,

u = linear growth rate of grains, cm/s .

The number of grains may be calculated by means of the following equation, suggested by Oldfield [8]:

$$N = \Phi * (\Delta T)^2 \quad (10)$$

where

Φ = nucleation coefficient, cm^3 ,

ΔT = undercooling, K , regarded as the difference between the liquidus temperature and the real temperature of a sample.

The crystal growth law [9] has also been used in the above calculations:

$$u = \mu * (\Delta T)^2 \quad (11)$$

where

μ = growth coefficient, $cm/(sK^2)$.

Results and discussion

Equations (6–11) were transformed into a differential form, and then combined with Eqs (2). The obtained set of equations was solved by means of the iteration method of secants, assuming an accuracy of computation $\delta \leq 0.005 K$.

Some computed temperatures are shown in Fig. 3.

The temperature under the reference is almost the same as that produced by the heater. However, the temperature evolution at the monitoring station differs significantly from that within the sample.

Therefore, it seemed of interest to consider the evolution of latent heat at the two compared sites. This is shown in Fig. 4.

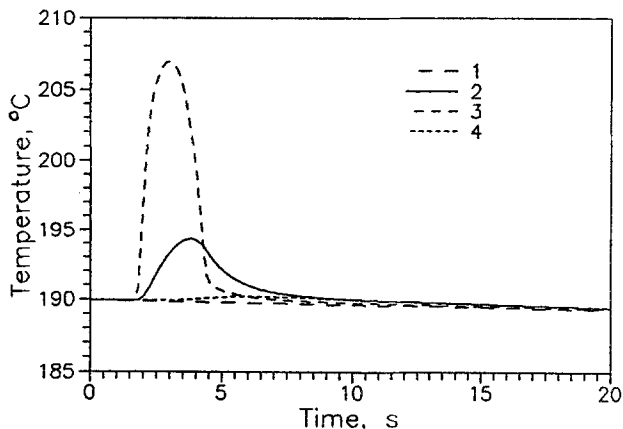


Fig. 3 Temperatures in the calorimeter cell: 1 – of the heater (T_1, T_7), 2 – at the monitoring station (T_2) (computed), 3 – within the sample (T_3) (computed), 4 – under the reference (T_5) (computed)

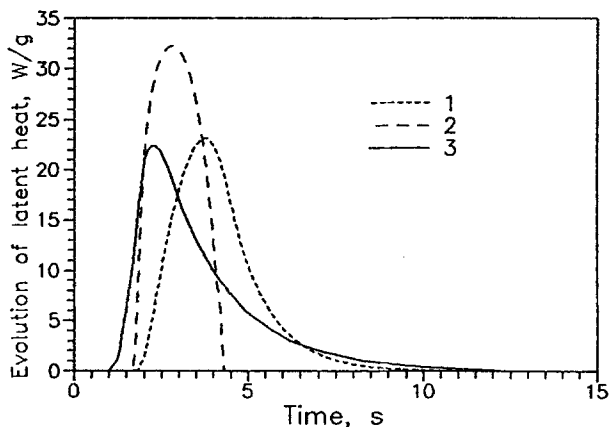


Fig. 4 Kinetics of latent heat for solidification of pure Sn: 1 – according to the temperature at the monitoring station (computer simulation), 2 – for real solidification within the sample (computer simulation), 3 – recorded experimentally, at a cooling rate of 2 deg/min [3]

The kinetics shown by curves 1 and 3 are almost identical, which proves that the proposed method of calculation is adequate for the heat-flux DSC method of measurements used in the experiment. However, the simulated kinetics of solidification (curve 2) differs significantly from that recorded at the monitoring station (curve 1).

The difference between the evolutions of temperature within the sample and at the monitoring station (curves 2 and 3 in Fig. 3) is also significant.

The discussed differences (Figs 3 and 4) are illustrated by the evolution of undercooling during solidification (Fig. 5).

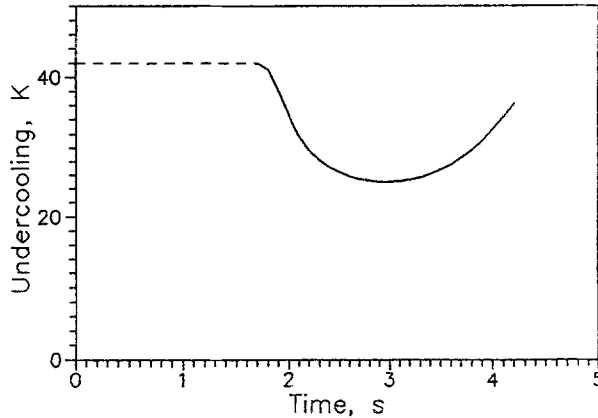


Fig. 5 Evolution of undercooling within a sample of pure Sn

The simulated parameter (Fig. 5) changes during the experiment after incubation for some time, whereas only one value of undercooling is available from the measurement. The assumed undercooling in the incubation period for pure Sn solidification at $u_0 = 2$ deg/min is 42 K.

The results of the considerations shown in Figs 3, 4 and 5 prove the importance of the simulation of the studied process for a given type of instrument. The need for analysis of the kinetics of the process within the sample instead of simple interpretation of the signal from the monitoring station is also emphasized.

References

- 1 S. C. Mraw, *Rev. Sci. Instrum.*, 53 (1982) 228.
- 2 Y. Saito, K. Saito and T. Atake, *Thermochim. Acta*, 99 (1986) 299.
- 3 A. L. Pulluard, *Rapport de Stage au CTM du CNRS, Marseille*, 1985/86.
- 4 E. Frás and W. Kapturkiewicz, (in:) *Physical Metallurgy of Cast Iron IV*, MRS, Pittsburgh, Pennsylvania, 1989, p. 469.
- 5 A. N. Kolmogorov, *Izv. AN SSSR*, 3 (1937) 355.
- 6 K. A. Johnson and R. Mehl, *Trans. AIME*, 135 (1939) 416.

7 M. Avrami, J. Chem. Phys., 7 (1939) 31.

8 W. Oldfield, Trans. ASM, 59 (1966) 945.

9 W. A. Tiller, (in:) Recent Research on Cast Iron, New York, 1968, p. 129.

Zusammenfassung — Es wird eine allgemeine mathematische Behandlung von Wärme- und DSC gegeben. Es verbindet Gleichungen für den Wärmetransport in der Kalorimeterzelle mit einer Annäherung der Verfestigung von Metall oder Legierung, die in diesem Gerätetyp durchgeführt werden. Es werden die Unterschiede zwischen: Temperaturevolution, Kinetik latenter Wärme und Unterkühlungsevolution innerhalb der Probe und zwischen: Temperaturevolution, aufgezeichnetes Signal und gemessene Unterkühlung an der Monitorstation diskutiert.